JOURNAL OF PLANKTON RESEARCH | VOLUME 33 | NUMBER 1 | PAGES 161–178 | 2011

Carbon biomass, elemental ratios (C:N) and stable isotopic composition (δ^{13}C, δ^{15}N) of dominant calanoid copepods during the winter-to-summer transition in the Amundsen Gulf (Arctic Ocean)

ALEXANDRE FOREST [1,2]*, VIRGINIE GALINDO [2], GÉRALD DARNIS [2], SIMON PINEAULT [2], CATHERINE LALANDE [2†], JEAN-ÉRIC TREMBLAY [2] AND LOUIS FORTIER [2]

[1]INSTITUT NATIONAL DE LA RECHERCHE SCIENTIFIQUE – EAU TERRE ENVIRONNEMENT, UNIVERSITÉ DU QUÉBEC, QUÉBEC, CANADA G1K 9A9 AND [2]QUÉBEC-OCÉAN, DÉPARTEMENT DE BIOLOGIE, UNIVERSITÉ LAVAL, QUÉBEC, CANADA G1V 0A6

[†]PRESENT ADDRESS: ALFRED WEGENER INSTITUTE, AM HANDELSHAFEN 12, D-27570 BREMERHAVEN, GERMANY

*CORRESPONDING AUTHOR: alexandre.forest@ete.inrs.ca, alforest@videotron.ca

Received April 21, 2010; accepted in principle July 22, 2010; accepted for publication July 24, 2010

Corresponding editor: Mark J. Gibbons

Calanoid copepods dominate mesozooplankton biomass in the Arctic Ocean. Variations in C content, C:N ratio and stable isotope composition (δ^{13}C, δ^{15}N) of *Calanus hyperboreus*, *Calanus glacialis* and *Metridia longa* collected from January to August 2008 in the southeast Beaufort Sea provided insights into their metabolism, feeding and reproduction. Seasonal differences in the C–prosome length relationships and C:N ratios were driven by distinct spawning strategies and changes in lipid content. Relatively high copepod biomass over the study period (2.6–9.7 g C m^{-2}) corresponded to favorable growth conditions in 2007–2008. The mean ^{15}N enrichment of copepods (+2.8–4.7‰) relative to particulate organic nitrogen values recorded at the ice bottom and at the chlorophyll maximum indicated a primarily herbivorous diet. In all species, δ^{13}C and δ^{15}N decreased markedly in April, reflecting the feeding onset on ice algae, but a rapid transition to feeding on phytoplankton occurred as a pelagic bloom was triggered by the early ice melt in May. A second decline in the δ^{13}C and δ^{15}N of copepods was recorded in June–July, coincident with a second increase in phytoplankton production. The two isotope depletion events in copepods were both followed by a return to high values and an increase in their C:N as a consequence of previous C fixation and nitrate limitation in phytoplankton and the likely formation of body reserves/tissue. Our results illustrate that Arctic calanoids respond quickly to any increase in primary production and can cope with changes in its nature and timing.

KEYWORDS: calanoid copepods; carbon biomass; stoichiometry; stable isotopes; Arctic Ocean

doi:10.1093/plankt/fbq103, available online at www.plankt.oxfordjournals.org. Advance Access publication August 21, 2010

INTRODUCTION

Communities of mesozooplankton in the Arctic Ocean are less diverse than at lower latitudes (Smith and Schnack-Schiel, 1990) and are typically dominated by copepods, both in terms of numerical abundance and biomass (e.g. Thibault *et al.*, 1999; Hopcroft *et al.*, 2005; Kosobokova and Hirche, 2009). Among copepods, the large calanoid *Calanus hyperboreus*, *Calanus glacialis* and *Metridia longa*, as well as *C. finmarchicus* in regions of major Atlantic water influence, usually account for 70–90% of mesozooplankton biomass (e.g. Arashkevich *et al.*, 2002; Ashjian *et al.*, 2003; Darnis *et al.*, 2008; Kosobokova and Hopcroft, 2010). Owing to this high proportion, *Calanus* spp. and *M. longa* are central components of Arctic marine food webs. While being able to feed on microzooplankton, eggs or detritus (Plourde and Joly, 2008; Campbell *et al.*, 2009; Sampei *et al.*, 2009), they are more traditionally known to exploit ice algae and phytoplankton for their growth and maturation (e.g. Hirche and Kosobokova, 2003; Seuthe *et al.*, 2007; Søreide *et al.*, 2008; Falk-Petersen *et al.*, 2009). *Calanus* spp. and *M. longa* are also the main observed prey of polar cod (*Boreogadus saida*) (Benoit *et al.*, 2010), which in turn is a key link for the trophic transfer of energy and nutrients to apex predators (e.g. Loseto *et al.*, 2008).

Arctic calanoid copepods are specialist organisms adapted to harsh environmental conditions, including subzero temperatures and a pronounced seasonality in light intensity and food availability. They have developed a variety of feeding and life-history strategies to survive in ice-covered waters (Conover and Huntley, 1991; Deibel and Daly, 2007; Falk-Petersen *et al.*, 2009). However, most of our knowledge on the dynamics of zooplankton communities in the Arctic Ocean comes from expeditions conducted in late summer and autumn, when sea ice extent is minimal (e.g. Mumm, 1991). As a result, zooplankton time series covering the winter-to-summer transition and based on direct plankton net sampling are scarce (e.g. Madsen *et al.*, 2001; Ashjian *et al.*, 2003; Forest *et al.*, 2008).

Over the last 30 years, significant trends toward earlier ice melt in spring and later freeze-up in autumn have been observed in the Arctic Ocean (Markus *et al.*, 2009). Furthermore, the melt season is increasingly dominated by thin first-year ice that is subject to seasonal melt (NSIDC, 2010). As these trends in Arctic sea ice regression persist (Wang and Overland, 2009), the intensity, nature and timing of micro-algal production are expected to change (Carmack and Wassmann, 2006). How will key zooplankton species respond to such changes is a critical issue for understanding potential shifts in energy and organic matter flows in Arctic marine ecosystems (e.g. Søreide *et al.*, 2010). Indeed, a central prerequisite of Arctic change research is to improve our understanding of ecosystem functionality, so that better predictive tools can be developed. In particular, possible impacts of climate-related changes in zooplankton communities include shifts in their biomass, stoichiometric composition and trophic interactions (e.g. Wiafe *et al.*, 2008; van de Waal *et al.* 2009; Drinkwater *et al.*, 2010). Such information can be provided by elemental and stable isotope measurements. Hence, baseline knowledge on these characteristics, and especially multi-season data sets, must be obtained before current environmental transitions transform the structure and function of Arctic marine ecosystems (*sensu* Carmack and Wassmann, 2006).

Here we report on the temporal variation of C–prosome length relationships, C:N ratios, stable isotopic signatures (δ^{13}C, δ^{15}N) and integrated C biomass of *C. hyperboreus*, *C. glacialis* and *M. longa* in the Amundsen Gulf (southeast Beaufort Sea, Arctic Ocean) from January to August 2008. Our main objectives were: (i) to supply adequate C–length equations for these species and to provide precise estimates of their biomass over the study period; (ii) to document the ranges of C:N ratios, δ^{13}C and δ^{15}N that occur in dominant Arctic copepods from winter to summer and to compare these ranges with those of particulate organic matter (POM) and (iii) to test for seasonal differences in the C–length relationships, C:N ratios and stable isotopes, in relation to the variation of sea ice conditions and surface layer temperature.

METHOD

Study area and spatial scope

The Amundsen Gulf is a large channel (~400 km length × 170 km width) that connects the southeast Beaufort Sea to the Canadian Archipelago (Fig. 1). Simplified water masses in the region comprise the Polar-Mixed Layer (salinity of ~26–31, 0–50 m) that sits over the Pacific Halocline (~32–33, 50–200 m), which itself overlays Atlantic Waters (≥34, >200 m) (Ingram *et al.*, 2008). Seasonal ice begins to form in October near the coasts and by late December the ice cover is consolidated (Galley *et al.*, 2008). Sea ice retreat has typically begun in early June with the widening of the flaw lead polynya complex close to Cape Bathurst (60% of the time), while in other years the ice break-up started later with a shore lead extending eastward from

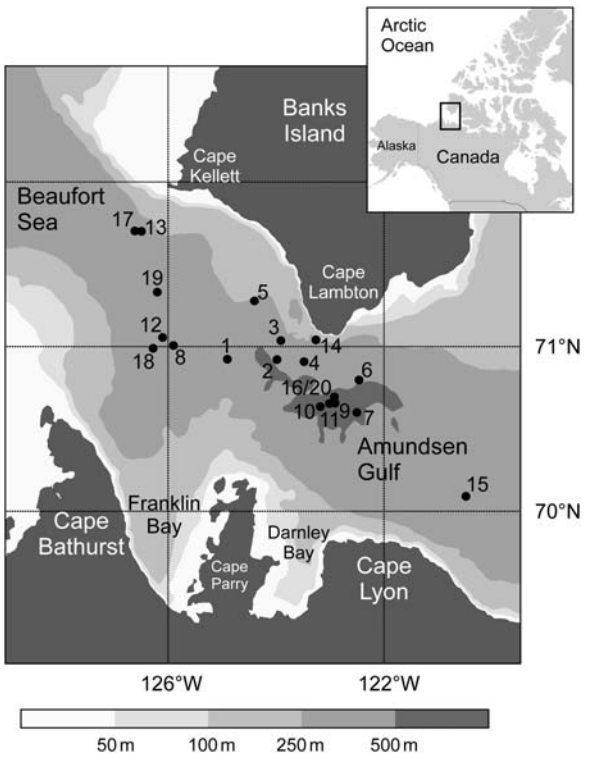

Fig. 1. Bathymetry of the Amundsen Gulf in the southeast Beaufort Sea (Arctic Ocean) with the position of stations where zooplankton and POM have been sampled from January to August 2008. The detail of sampling stations is given in Table I.

Cape Parry (Galley *et al.*, 2008). Ocean color remote sensing revealed that marked inter-annual variability in surface carbon pools is a key feature of the Amundsen Gulf/Cape Bathurst polynya region (Arrigo and van Dijken, 2004; Forest *et al.*, 2010).

We focused our study on the central Amundsen Gulf as defined as the area between 120 and 127°W with a bottom depth >250 m (Fig. 1). In this manner, relative homogeneity in the vertical extent and physical/biological properties of the water column could be obtained. This environment is recognized to be dominated by marine autochthonous processes in contrast to the adjacent coastal areas (e.g. Magen *et al.*, 2010; Morata *et al.*, 2008). Moreover, the zooplankton assemblage in the Amundsen Gulf polynya (250–537 m) was previously determined as being statistically similar, in particular with *C. hyperboreus* and *M. longa* as indicator species of this region (Darnis *et al.*, 2008). We thus assumed that the ecological setting was adequately delineated in order to investigate the temporal variability of biochemical properties of the three target copepods using pooled analyses from various stations located across the Amundsen Gulf.

Sea ice, temperature and chlorophyll fluorescence

Time series of weekly averaged ice concentrations and various stages of development (first-year and new/young sea ice) from January to August 2008 in the Amundsen Gulf were obtained with the Ice Graph Tool of the Canadian Ice Service (http://ice-glaces.ec.gc.ca/IceGraph/). The specific regions "Amundsen Gulf" [cwa05_01] and "Amundsen Gulf Mouth" [cwa05_03] were used to produce a spatial composite of ice concentrations across the study area. Ice concentration data were processed to exclude coastal sectors, such as the Franklin and Darnley bays.

A caged rosette profiler equipped with a conductivity–temperature–depth system (CTD, Seabird SBE-911+) and a fluorometer (Seapoint) was deployed at each sampling station (Fig. 1, Table I). The CTD data were calibrated and verified following the Unesco Technical Papers (Crease, 1988). The fluorescence data were calibrated against *in situ* chlorophyll *a* concentrations using linear regressions ($r^2 > 0.8$) kindly provided by J. Martin (Université Laval, Québec City, Canada). Validated temperature and fluorescence data were averaged over the 0–80 m interval to provide an overview of temperature and phytoplankton biomass in the surface layer throughout the study period.

Zooplankton sampling and taxonomy

Zooplankton was collected during the Circumpolar Flaw Lead System Study (CFL) aboard the CCGS *Amunsden* from January to August 2008 in the southeast Beaufort Sea (Fig. 1). The ship stayed mobile throughout this period following a semi-Lagrangian approach (see Barber, 2009 for details). Mesozooplankton was sampled using a 1 m^2 metal frame rigged with a 200 μm mesh net and equipped with a TSK flow meter for volume measurements. The gear was deployed vertically from 10 m off the bottom to the surface. Sampling at stations 1–8 (Table I) was performed through the moonpool of the ship due to ice cover conditions. Beginning on 19 May, sampling switched from moonpool to on-deck operations. At each station, one zooplankton net sample was preserved in seawater solution with borax-buffered 4% formaldehyde for taxonomic analysis. A second zooplankton sample was gently sieved, rinsed and stored in cryovials and frozen at −80°C for elemental and stable isotope analyses.

Samples for taxonomy were rinsed with freshwater and fractionated on 1000 and 177 μm mesh sieves to separate large and small organisms. The two size fractions were divided with a Folsom-type splitter and

Table I: Locations and sampling dates of stations used in the present study

Date	Station (Fig. 1)	CFL station ID	Latitude (°N)	Longitude (°W)	Bottom depth (m)	Sampling depth (m)
27 Jan	1	D19-6/7	70°55.50′	124°53.90′	315	305
26 Feb	2	D26-7	70°55.33′	123°58.95′	377	365
10 Mar	3	D29-13	71°02.31′	123°54.62′	321	314
17 Mar	4	D29-24	70°54.50′	123°26.60′	401	385
7 Apr	5	D36-4/5	71°16.70′	124°24.30′	258	244
15 Apr	6	D40-41	70°47.90′	122°27.80′	473	460
27 Apr	7	D43A	70°35.97′	122°30.12′	553	528
4 May	8	D43-23	71°00.46′	125°54.01′	408	381
19 May	9	405b	70°39.42′	122°54.39′	528	515
1 Jun	10	405c	70°38.19′	123°10.67′	540	501
10 Jun	11	405b1	70°39.28′	123°00.75′	611	600
28 Jun	12	1208	71°03.45′	126°05.83′	403	393
8 Jul	13	410	71°42.11′	126°29.79′	403	393
11 Jul	14	1100	71°02.62′	123°15.94′	270	260
20 Jul	15	403	70°05.45′	120°28.66′	411	401
21 Jul	16	405	71°41.70	122°55.50	599	580
23 Jul	17	437	71°42.23′	126°37.60′	439	430
26 Jul	18	CA08-07	70°59.37′	126°06.58′	398	385
2 Aug	19	2008	71°19.98′	126°11.79′	441	430
3 Aug	20	CA18-07	70°41.74′	122°54.94′	591	580

The station ID from the Circumpolar Flaw Lead (CFL) field expedition is also given in association with each station number.

Table II: Medians and ranges (i.e. min–max) of prosome lengths (mm) of the three target copepods

	C. hyperboreus		*Calanus glacialis*		*M. longa*	
Stage	Median	Range	Median	Range	Median	Range
♀	6.70	±0.80	4.10	±0.70	2.85	±0.35
♂	5.15	±0.25	3.80	±0.35	2.10	±0.20
CV	5.00	±0.60	3.40	±0.65	2.05	±0.25
CIV	3.85	±0.35	2.45	±0.45	1.50	±0.30
CIII	3.05	±0.45	1.70	±0.30	0.95	±0.20
CII	2.05	±0.55	1.25	±0.25	0.75	±0.20
CI	1.25	±0.25	0.80	±0.20	0.60	±0.15

All units are in mm.

known aliquots were resuspended in distilled water. The small fraction was diluted in 500 mL water and an appropriate number of subsamples were collected with a Henson-Stempel pipette. From each subsample, approximately 300 animals were counted and identified to species or to the lowest possible taxonomical level. Copepodite stages were determined according to their morphology and prosome length (Table II). The Arctic species *Calanus glacialis* and the Pacific sub-Arctic *Calanus marshallae* that may co-occur in the region (Frost, 1974) were pooled in a single taxon due to lack of certainty in their differentiation (Seuthe *et al.*, 2007; Darnis *et al.*, 2008).

POM sampling

POM was sampled at the bottom of the ice (7–27 April) and in the upper water column (7 April to 2 August) for the determination of C:N and stable isotope composition of copepod's food source. At each ice station, bottom-ice POM (0–10 cm) was obtained using pooled samples from 3 to 10 ice cores taken with a manual corer (Mark II coring system, 9 cm internal diameter, Kovacs Enterprise). Ice core samples were cut directly on the ice and put in a dark isothermal container prior to their transport back to the ship. Filtered seawater (0.7 μm) was added to the cores to minimize osmotic stress during melting (Garrison and Buck, 1986). Melted ice cores were pooled together for filtration onto 24 mm pre-combusted Whatman GF/F filters (0.7 μm). Pelagic POM samples were collected at 30 m depth (7–15 April) and thereafter at the depth of the chlorophyll maximum (16–56 m) with the onboard CTD rosette system. At each station, a minimum of 12 L was filtered onto 47 mm pre-combusted Whatman GF/F filters. All filters (bottom-ice and pelagic POM) were dried at 60°C for at least 24 h and stored with desiccant before being analysed for C:N and stable isotopes.

Elemental and stable isotope analyses

Copepodite stages (CI–CV) and adults of *C. hyperboreus*, *C. glacialis* and *M. longa* were sorted in multiple replicates from the collection of station-specific frozen zooplankton samples (Table I). Sorting was performed under a Leica MZ 7.5 dissecting stereo-microscope (magnification 10–200×) to allow the measurement of prosome length. Samples were kept over an ice bath (4°C) to prevent degradation.

For elemental analyses, whole and intact organisms were picked, pooled if necessary to obtain sufficient material (up to six individuals), placed into pre-weighed tin cups (Perkin Elmer standard size 5 × 9 mm) or on pre-weighed Whatman glass fiber filters (GF/F, 0.7 μm) and dried at 60°C for more than 24 h. After drying, tin cups and GF/F were weighed again for the determination of copepod dry weight (DW) using a Sartorius ME5 microbalance (precision ±1 μg). Tin cups and GF/F folded into tin cups were burned at 925°C in a Perkin Elmer CHN 2400 Series II Elemental Analyzer (accuracy <0.3% and precision <0.2%) to measure the C and N content of copepods.

For stable isotope analyses, a second subset of copepods (CIV–V and adult females) was sorted, dried, weighed and placed in tin cups as described above. We selected only these stages in order to determine the mean δ^{13}C and δ^{15}N of each copepod species using the stages that typically dominate the biomass. Large copepod specimens (>3 mm prosome length) were ground to a fine powder and divided into two to four cups consistent with the maximum detection limit of the stable isotope analyzer. Ratios of $^{13}C/^{12}C$ and $^{15}N/^{14}N$ were determined using a mass spectrometer (Thermo Finnigan DeltaPlus Advantage) in the continuous-flow mode (ConFlo III), equipped with a high-temperature elemental analyzer. Stable isotope ratios of C and N are described as a per mil (‰) deviation from the respective international standards, using the following equation:

$$\delta X = \left[\frac{R_{\text{sample}}}{R_{\text{standard}}} - 1\right] \times 1000,$$

where X represents ^{13}C or ^{15}N and R is the $^{13}C/^{12}C$ or $^{15}N/^{14}N$ ratio, respectively. L-Glutamic acids (USGS40 and USGS41, US Geological Survey, Reston, VA, USA) calibrated against Peedee-Belemnite and atmospheric N_2 were used as international organic references for stable isotope analyses (Qi *et al.*, 2003). Analytical grade acetanilide was used to calibrate the quantification of C and N. Lipids were not extracted prior to stable isotope analyses to prevent any impact on the δ^{15}N, which may be altered following the loss of some non-lipid compounds during extraction (e.g. Sweeting *et al.*, 2006). Hence, the δ^{13}C of copepods were corrected for lipids using the mass balance model recommended by Smyntek *et al.* (2007) for zooplankton [see their equation (5)]. Such a mathematical model based on C:N ratios of specific biological material is increasingly recognized as a reliable alternative to chemical extraction correction (Logan *et al.*, 2008).

The bottom-ice and pelagic POM samples were analysed on the same mass spectrometer as the one used for copepod measurements and using the same analytical procedure. No post-analysis correction on the elemental and stable isotope ratios of POM was applied.

Data analyses

The individual C contents of copepods were related to the individual prosome lengths to construct seasonal power-law C–length relationships ($y = ax^k$) as described in Ashjian *et al.* (Ashjian *et al.*, 2003). Results of C measurement from both elemental analyzers were combined to increase the number of data available to produce the C–length relationships. Coincidence between the seasonal C–length equations was tested with pairwise analyses of covariance (ANCOVASs) performed on log-transformed C contents and prosome lengths. The ANCOVAs made use of log(C content) as the dependent variable, log(prosome length) as the co-variable and the season (winter, spring, summer) as the factor [see Sokal and Rohlf, (1995) for details]. Thus, testing for significance of the sources of variation "season" and "log(prosome length)*season" corresponded, respectively, to testing for differences in the multiplier constant (a) and the scaling exponent (k) between two C–length relationships. Hence, if at least one of these sources of variation was significant, both compared power-law relationships were considered statistically different.

Seasonal differences between mean C:N ratios, δ^{13}C and δ^{15}N in copepods were tested using one-way analyses of variance (ANOVAs) followed by *post hoc* Tukey's HSD (honestly significant difference) multiple comparison tests. For each tested data set, assumption for normality prior to ANOVAs was verified using the Shapiro–Wilk test ($P < 0.05$). Non-normal distributions were log- or square-root-transformed in order to reject the null hypothesis that the data were not from a normally distributed population. All statistical analyses and tests were performed at a level of significance $\alpha < 0.05$ using the SYSTAT Software Package (V.12, www.systat.com).

RESULTS

Sea ice, temperature and chlorophyll fluorescence

Throughout the study period in 2008, sea ice concentration in the central Amundsen Gulf never reached

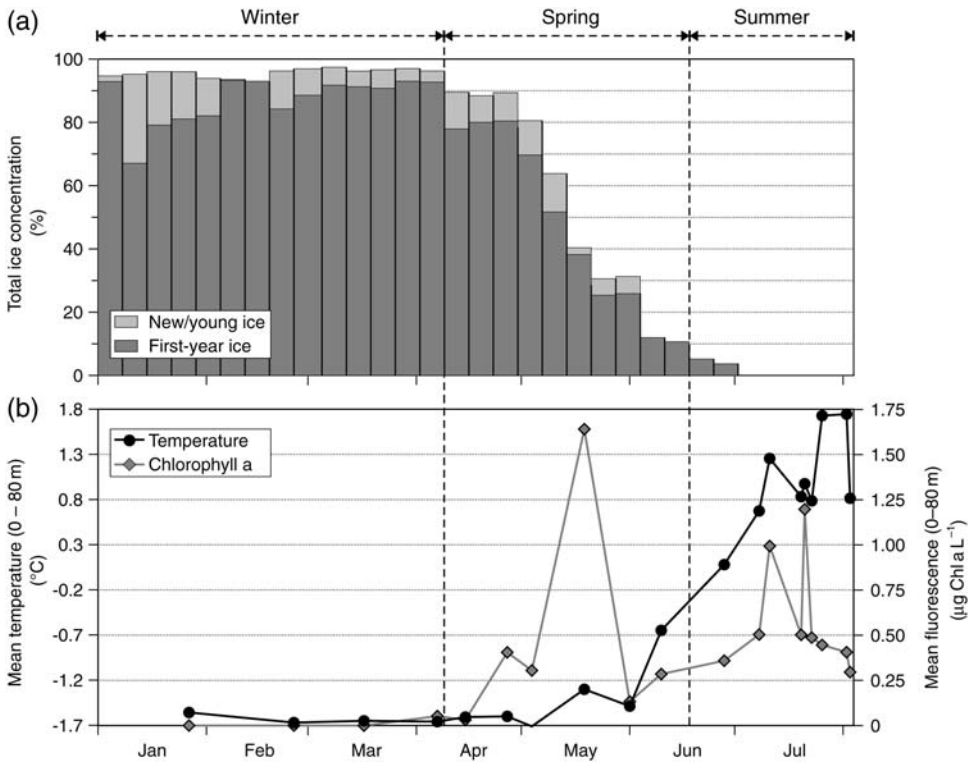

Fig. 2. Time series of **(a)** weekly sea ice concentration (% cover) in the central Amundsen Gulf divided into two stages of development and **(b)** mean temperature and chlorophyll fluorescence concentration over the 0–80 m water layer at each sampling station (Fig. 1 and Table I). Based on the evolution of sea ice conditions and temperature records, we separated the study period in three seasonal intervals. The winter corresponds to $T^\circ < 0^\circ$C and ice >90%; the spring to $T^\circ < 0^\circ$C and ice <90% and the summer to $T^\circ > 0^\circ$C and ice <10%.

100% in total sea area and declined sharply from ~90% in mid-April to ~10% in mid-June (Fig. 2a). Weekly ice concentrations were dominated by first-year sea ice, but the total sea area often comprised a fair amount (up to 28%) of new/young ice. This likely indicated that the ice cover was dynamic and that newly exposed leads were frequently re-freezing until May.

Calibrated temperature and fluorescence concentrations averaged within the 0–80 m surface layer exhibited distinct temporal patterns (Fig. 2b). Mean temperature in the upper water column remained below 0°C until mid-June and increased up to ~1.8°C when sea ice melted completely in July. Chlorophyll fluorescence remained at nil values until mid-April and peaked in May (~1.7 µg Chl $a\,L^{-1}$) concomitantly with the intense melt period. After a marked decline in early June, mean fluorescence increased again in July (up to ~1.2 µg Chl $a\,L^{-1}$). Over the productive period, the chlorophyll maximum progressively deepened from 16 m in late April down to 56 m depth in early August (not shown).

Changes in total ice concentration and surface layer temperature were used as criteria to define the seasonal intervals. The winter period would correspond to $T^\circ <$ 0°C and ice >90%; the spring to $T^\circ < 0^\circ$C and ice $\leq$90% and the summer to $T^\circ \geq 0^\circ$C and ice $\leq$10% (Fig. 2).

Seasonal variability of individual carbon content and integrated C-biomass

From winter to summer 2008, the percentage of C in DW was similar ($r^2 > 0.94$, $P < 0.0001$) among individual copepods (Fig. 3). The highest mean C content was measured in the large *C. hyperboreus* (63%), but C was also the dominant element of the average DW biomass of *C. glacialis* (59%) and *M. longa* (54%). Given the high similarity of C content in each species, we decided to not show the relationships between DW and prosome lengths and to focus thereafter on the individual C contents and C–length equations.

Within each of the three seasonal intervals, the regressions of individual C contents on prosome lengths resulted in significant power-law relationships (r^2 from 0.65 to 0.89, $P < 0.001$) for every copepod species (Fig. 4). ANCOVAs performed between seasonal C–length relationships revealed, however, that there were no statistical differences for *M. longa* among

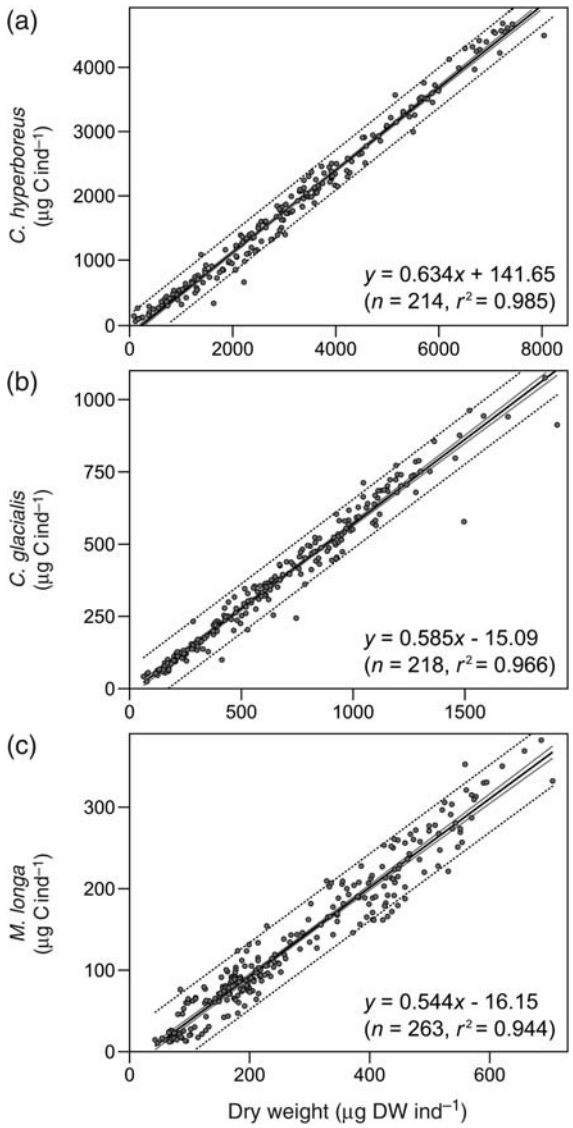

Fig. 3. Linear regressions of individual C content against individual DW for each of the studied copepod species: **(a)** *C. hyperboreus*, **(b)** *C. glacialis* and **(c)** *M. longa*. The three regressions include all the data obtained for the entire study period from January to August 2008.

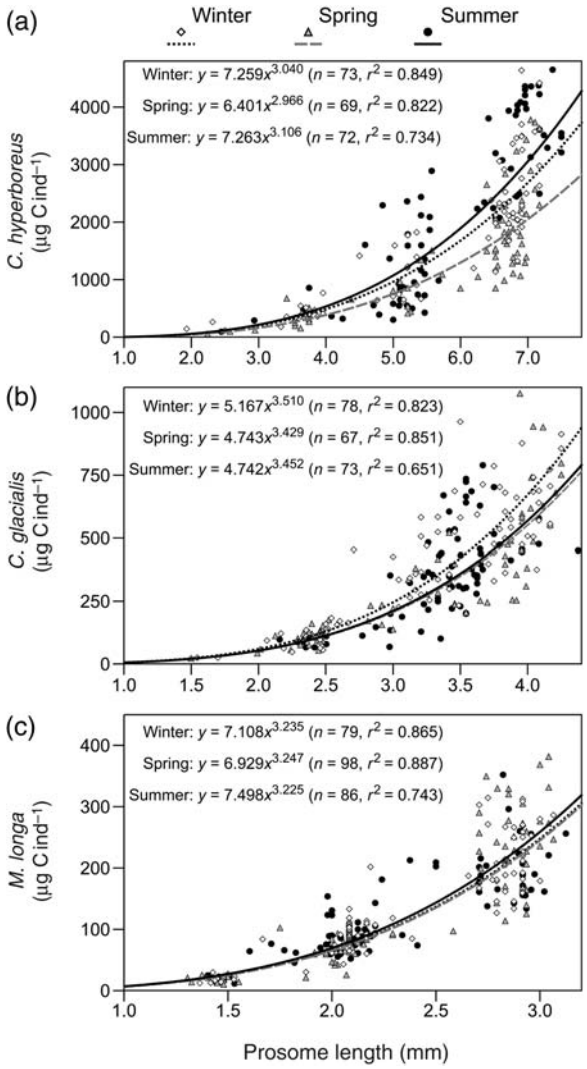

Fig. 4. Relationships between individual C-content and prosome length for each of the studied copepod species: **(a)** *C. hyperboreus*, **(b)** *C. glacialis*, and **(c)** *M. longa*. The datasets have been divided into three seasons according to the variation of sea ice conditions and surface layer temperature records (Fig. 2) in order to obtain distinct best-fit power equations.

seasons and that similarities occurred between winter and summer for *C. hyperboreus*, and between spring and summer for *C. glacialis* (Table III). Accordingly, it is possible to group the similar data sets in order to produce a single equation for these periods as presented in Table IV.

Differences in the power-law equations of the two *Calanus* species were driven by temporal changes in the C content of stages CV and/or adult females (Fig. 5). In *C. hyperboreus*, the low C contents of adult females in April (Fig. 5a) were responsible for the significantly low power-law parameters of the spring equation (Fig. 4a, Table III). In *C. glacialis*, and despite strong individual variability, the combination of relatively high C content of stages CV and adult females from January to March (Fig. 5b) resulted in a significantly high multiplier constant in the winter equation (Fig. 4b, Table III). In contrast, the marked monthly variations in the C content of adult females of *M. longa* (Fig. 4c) did not give rise to any difference in the seasonal C–length relationships (Table III).

The determination of specific regional and seasonal C–length relationships for *C. hyperboreus*, *C. glacialis* and *M. longa* enabled us to transform the integrated abundance of these species into precise estimates of their C biomass (Fig. 6). Overall, the large *C. hyperboreus*

Table III: Results of the ANCOVAs performed to test the coincidence of C–length relationships presented in Fig. 4

		C. hyperboreus				*Calanus glacialis*				*M. longa*			
ANCOVA	Source of variation in the power-law relationship	Sum of squares	Mean square	Fisher's *F*	Pr > F	Sum of squares	Mean square	Fisher's *F*	*P* > F	Sum of squares	Mean square	Fisher's *F*	*P* > F
Winter and spring	Prosome length (*x*)	415.42	415.42	21 882.14	<0.001	369.56	369.56	21 061.30	<0.001	256.14	256.14	16 083.08	<0.001
	Multiplier constant (*a*)	0.38	0.38	19.92	**<0.001**	0.18	0.18	10.21	**0.002**	0.00	0.00	0.23	0.633
	Scaling exponent (*k*)	0.06	0.06	3.31	0.071	0.05	0.05	2.86	0.092	0.00	0.00	0.06	0.802
Winter and summer	Prosome length (*x*)	436.57	436.57	17 117.08	<0.001	376.31	376.31	17 419.60	<0.001	250.44	250.44	16 872.48	<0.001
	Multiplier constant (*a*)	0.05	0.05	2.07	0.152	0.15	0.15	7.04	**0.009**	0.02	0.02	1.53	0.218
	Scaling exponent (*k*)	0.05	0.05	1.99	0.161	0.03	0.03	1.24	0.267	0.00	0.00	0.04	0.851
Spring and summer	Prosome length (*x*)	426.65	426.65	16 367.18	<0.001	357.67	357.67	17 006.74	<0.001	249.15	249.15	15 057.61	<0.001
	Multiplier constant (*a*)	0.71	0.71	27.35	**<0.001**	0.00	0.00	0.10	0.751	0.05	0.05	2.90	0.090
	Scaling exponent (*k*)	0.23	0.23	8.69	**0.004**	0.00	0.00	0.18	0.672	0.00	0.00	0.18	0.674

The power-law equations ($y = ax^k$) are considered similar only if both the multiplier constant (*a*) and the scaling exponent (*k*) are non-significant within a 95% confidence interval. If at least one of the power-law parameters is significant, the two compared relationships are considered statistically different (results in bold). The ANCOVAs were performed using log-transformed carbon contents and prosome lengths in order to linearize the power-law relationships.

Table IV: Power-law equations relating the C content (C) to prosome length (L) of the three target copepods using statistically similar seasonal data sets

	C. hyperboreus	*Calanus glacialis*	*M. longa*
Winter	[a] $C = 7.258L^{3.074}$	[b] $C = 5.167L^{3.510}$	$C = 7.168L^{3.236}$
Spring	[b] $C = 6.401L^{2.966}$	$C = 4.744L^{3.441}$	
Summer	[a] $C = 7.258L^{3.074}$		

The ANCOVAs (Table III) performed between the seasonal C–length relationships (Fig. 4) revealed that there were no statistical differences for *M. longa* among seasons and that similarities occurred between winter and summer for *C. hyperboreus* and between spring and summer for *C. glacialis*. Prosome length is expressed in mm. Carbon content is expressed in μg C ind^{-1}.

[a]Same equation.

[b]From Fig. 4.

represented only 6% of the total abundance, but accounted for 48% of the summed biomass of the three copepods. The most abundant species was *M. longa* (56%) which represented 20% of the C biomass. *Calanus glacialis* accounted for 38 and 32% of the total abundance and C biomass, respectively. From winter to summer 2008, the total abundance of the three copepod species in the central Amundsen Gulf decreased significantly over time (Fig. 6a). This was mainly due to a pronounced decline in stages CI–III of *M. longa* and *C. glacialis* that were progressively replaced by a higher proportion (but less abundant) of CIV–V over the study period (Table V). A shift from CIV to CV in the relative stage composition of *C. hyperboreus* can also be detected over spring (Table V). Accordingly, the seasonal variation of copepod C biomass exhibited an apparent bimodal pattern, with a negative trend in winter and a positive trend in spring-summer (Fig. 6b). However, these trends were not significant at $P < 0.05$ due to not enough data points. When averaged over the study period, adult *C. hyperboreus* (♀ at 98%) and stages CIV–V of *C. glacialis* contributed, respectively, to 37 and 25% of the total biomass. Stages CIV–V of *C. hyperboreus* as well as stages CIV–V and adults of *M. longa* contributed to ~10% each, while the contribution of stages CI–III and adult *C. glacialis* were ~3% each. The low percentage of *C. glacialis* adults in total biomass resulted from a low proportion (1–6%) of *C. glacialis* females in the abundance of this species (Table V). Stages CI–III of *C. hyperboreus* and *M. Longa* contributed ≤1% each to total biomass.

Temporal variations of C:N ratios and stable isotopes in copepods and POM

From late January to early August 2008, C:N ratios, $\delta^{13}C$ and $\delta^{15}N$ of the three target copepods (pooled

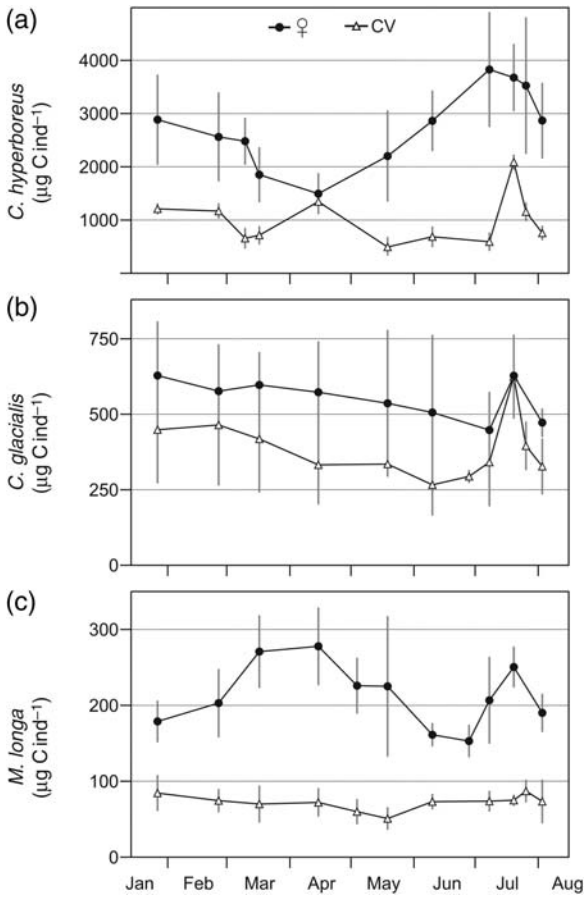

Fig. 5. Time series of individual C-content of adult females and copepodite stages CV for each of the studied copepod species during the winter-to-summer transition in 2008: **(a)** *C. hyperboreus*, **(b)** *C. glacialis*, and **(c)** *M. longa*. The vertical gray bars depict the standard deviations.

stages CIV–V and adult females) exhibited marked amplitudes and the temporal variations clearly exceeded the inter-individual variability (Fig. 7). Stages were pooled for convenience to show the mean (±standard deviation) stoichiometric and stable isotopic signals of a given species using the stages that generally dominated the C biomass (Fig. 6, Table V). Above all, it is worth mentioning that the most striking patterns were observed in March–April, and to a lesser extent in June–July, when quasi-concomitant shifts from relatively high-to-low values of C:N, δ^{13}C and δ^{15}N were observed in every copepod species. These shifts, however, did not necessarily result in statistical differences between mean seasonal elemental or stable isotopic ratios (Table VI).

The lowest mean C:N ratios in copepods (down to ~3–5) were observed from mid-April to early May (Fig. 7a–c), but the Tukey's tests revealed significantly low C:N ratios in spring for *C. glacialis* only (Table VI). In other seasons, the mean C:N remained generally between 6 and 10, except for early June, when simultaneous peaks up to 12 were measured in *C. glacialis* and *M. longa*. High C:N ratios (>10) were also measured in *M. longa* in late July–early August (Fig. 7c), a species that showed as well higher mean C:N ratios than the two *Calanus* spp. in all seasons (Table VI). In spring and summer, the C:N ratio of POM ranged from ~5 to ~11 (Fig. 8a), thus exhibiting lesser variability than the C:N of copepods (Fig. 7a–c). The temporal pattern of C:N in POM was different from that of copepods, such as the lack of pronounced decline in the C:N of POM in mid-April, and the absence of marked increase in late May and late July. The mean C:N of bottom-ice POM (9.0) was higher than that recorded in the upper water column (6.8).

The mean δ^{13}C values of copepods ranged from −25.5 to −20.8‰ (Fig. 7d–f), with lowest values in mid-April (*M. longa*) or early May (*C. hyperboreus* and *C. glacialis*) and highest values in mid-March (*C. glacialis*), late May (*C. hyperboreus*) or early June (*M. longa*). Tukey's tests determined that the mean seasonal δ^{13}C were higher in winter (> − 22.0‰) than in spring–summer for *C. hyperboreus* and *C. glacialis*, while no seasonal difference was found in *M. longa* (Table VI). In spring–summer, the mean δ^{13}C of *M. longa* remained relatively high (approximately −22.0‰) compared with its mean winter value (Table VI). The δ^{13}C signals of POM were systematically lower than those of copepods and oscillated between 31.1 and −24.4‰ (Fig. 8b). The highest δ^{13}C values were measured at mid-April in bottom-ice POM and at mid-May and in July in pelagic POM (Fig. 8b). All these three maxima were preceded by a steep increase from relatively low δ^{13}C values. The highest δ^{13}C values in pelagic POM were recorded at the same time as the peaks in the chlorophyll biomass were detected (Fig. 2b).

As for the δ^{15}N in copepods, the lowest values (~5.0‰) were observed in mid-April for *C. hyperboreus* and *M. longa* and in early May for *C. glacialis* (Fig. 7g–i). The highest δ^{15}N values in copepods (16–19‰) were also detected in springtime, roughly 4–8 weeks later, i.e. with *M. longa* and *C. glacialis* in early June, and *C. hyperboreus* in mid-June. Tukey's tests showed, as for the C:N and δ^{13}C analyses, no seasonal difference in the mean δ^{15}N of *M. longa* during the winter-to-summer period (Table VI). In *C. hyperboreus*, the mean δ^{15}N was statistically higher in summer than in winter and spring, whereas in *C. glacialis*, the mean δ^{15}N in summer was also significantly higher than in spring, but not when compared with the mean δ^{15}N in winter (Table VI). The δ^{15}N of bottom-ice and pelagic POM remained at similarly low values in April–May (4.6–6.7‰), but a

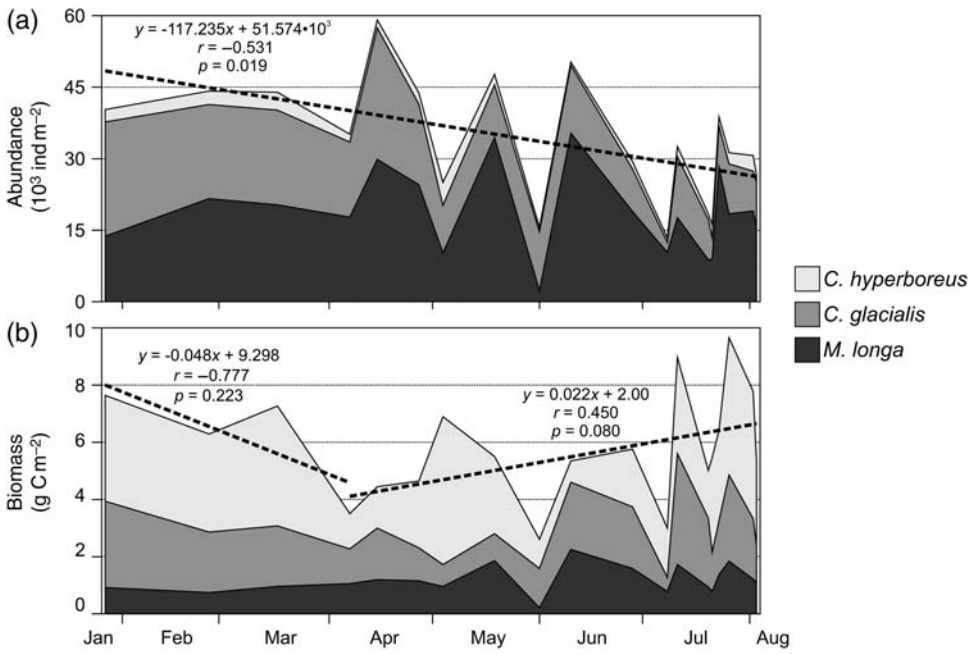

Fig. 6. Seasonal evolution of integrated **(a)** abundance and **(b)** C biomass of *C. hyperboreus*, *C. glacialis* and *M. longa* sampled from January to August 2008 in the central sector of the Amundsen Gulf (Fig. 1 and Table I). The successive C biomasses were calculated using the seasonal C–length power-law relationships presented in Fig. 4. The details of the relative stage composition in the total abundance and biomass of each species are presented in Table V.

marked increase up to ~12‰ was observed in the pelagic POM throughout June (Fig. 8c). This increase was concomitant with the decline in the chlorophyll biomass (Fig. 2b). A return to low $\delta^{15}N$ values in POM (~6‰) was observed in early July as peaks in chlorophyll fluorescence were observed again.

DISCUSSION

The seasonal variability in the individual C content and C–length relationships of dominant calanoid copepods

Precise measurements of individual C content of copepods are critical for estimates of total biomass based on total abundance (Hopcroft *et al.*, 2005) as well as for empirical estimates of growth rates (Hirst and Bunker, 2003). Given the various life-history strategies of Arctic calanoids (Conover and Huntley, 1991; Falk-Petersen *et al.*, 2009), the relationships between their C content and body length are expected to vary between seasons. In the present study, the specific C–length relationships constructed for winter, spring and summer aim at supplying a specific data set for dominant calanoid copepods in the southeast Beaufort Sea. Previously, the equations of Ashjian *et al.* (Ashjian *et al.*, 2003) for *Calanus* spp. and those of Mumm (Mumm, 1991) for *M. longa* (both constructed with samples from the central Arctic basins) were used in our study region. However, no seasonal distinctions were made in these studies to take into account the different metabolic, feeding and reproduction patterns of Arctic calanoids.

For example, we know that *C. hyperboreus* starts to spawn in winter, does not rely on external food sources to produce eggs and loses a substantial amount of lipids before spring until females are spent (Head *et al.*, 1985; Conover and Huntley, 1991; Seuthe *et al.*, 2007). Obviously, this characteristic caused the low individual C content of *C. hyperboreus* females in April, which gave rise to a significantly low multiplier constant in the spring equation compared with winter and summer (Table III). Then, at the onset of the productive season, this species is adapted to feed actively on phytoplankton in order to accumulate lipid reserves over the summer and maximize its condition before diapause (Deibel and Daly, 2007; Falk-Petersen *et al.*, 2009). As a result, both the multiplier constant and the scaling exponent of the C–length equation of *C. hyperboreus* were higher in summer than in spring.

In contrast, *C. glacialis* remains inactive during winter and reacts promptly to the beginning of the ice algal production by starting to feed and spawn (Runge and Ingram, 1991; Fortier *et al.*, 2002; Hirche and

Table V: Average monthly fraction of copepodite and adult stages in the abundance (ab) and biomass (bio) of C. hyperboreus, C. glacialis and M. longa from January to August 2008 in the central Amundsen Gulf

		January		February		March		April		May		June		July		August	
		ab	bio	ab	bio	ab	bio	ab	bio	ab	bio	ab	bio	ab	bio	ab	bio
C. hyperboreus	♀	49	81	39	78	35	79	35	76	50	82	40	69	42	73	42	73
	♂	5	4	—	—	2	2	2	2	—	—	1	1	—	—	—	—
	CV	10	7	7	6	3	3	7	6	20	14	33	25	32	24	31	22
	CIV	28	7	52	16	43	15	43	15	10	3	13	3	10	2	15	4
	CIII	8	1	2	0	7	<1	4	<1	10	1	12	1	8	1	7	1
	CII	—	—	—	—	5	<1	3	<1	2	<1	<1	<1	3	<1	2	<1
	CI	—	—	—	—	5	<1	6	<1	7	<1	<1	<1	6	<1	6	<1
C. glacialis	♀	6	30	2	10	4	25	1	11	1	4	3	11	1	2	2	4
	♂	—	—	2	8	<1	2	<1	3	<1	4	<1	1	<1	1	—	—
	CV	6	16	2	7	2	6	<1	4	2	9	41	61	87	95	60	93
	CIV	34	32	49	54	39	44	29	41	50	62	35	24	4	1	2	1
	CIII	55	22	45	21	50	23	67	41	40	21	7	2	1	<1	3	1
	CII	—	—	—	—	4	<1	1	<1	2	<1	3	<1	2	<1	4	<1
	CI	—	—	—	—	—	—	1	<1	4	<1	9	<1	5	<1	29	<1
M. longa	♀	29	90	10	61	9	39	6	23	18	46	16	44	19	46	10	33
	♂	3	3	2	5	3	5	3	4	8	8	6	6	8	7	8	9
	CV	2	2	5	11	17	27	30	42	29	29	48	43	48	42	46	52
	CIV	2	<1	16	12	46	26	53	30	41	17	16	6	11	5	12	5
	CIII	26	2	52	9	21	3	6	<1	4	<1	3	<1	3	<1	7	<1
	CII	35	1	13	1	3	<1	2	<1	<1	<1	4	<1	7	<1	5	<1
	CI	3	<1	2	<1	1	<1	1	<1	—	—	6	<1	4	<1	13	<1

This table aims at providing the detailed relative stage composition in the total abundance and biomass of the three target copepods presented in Fig. 6.

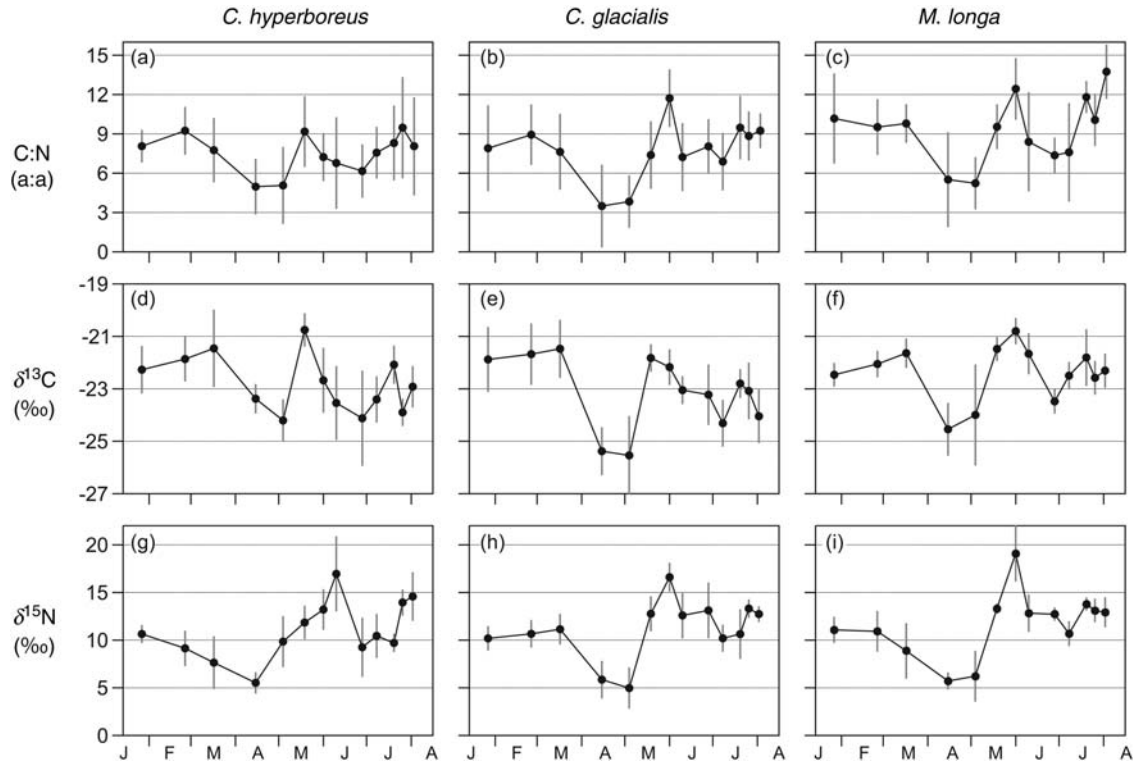

Fig. 7. Time series of **(a–c)** C:N ratios, **(d–f)** δ^{13}C and **(g–i)** δ^{15}N for each of the studied copepod species in the Amundsen Gulf from January to August 2008. This data set represents pooled results from analyses on stages CIV-V and adult females in order to present the mean isotopic signal of a given species using the stages that generally dominated the biomass (Table V). The vertical gray bars depict the standard deviations.

Table VI: Seasonal means and standard deviations (SD) of C:N ratios, $\delta^{13}C$ and $\delta^{15}N$ signatures of the three copepod species obtained via one-way ANOVAs

		C. hyperboreus			*Calanus glacialis*			*M. longa*		
		Mean	SD	Tukey's Grouping	Mean	SD	Tukey's Grouping	Mean	SD	Tukey's Grouping
C:N ratio	Winter	7.81	0.29	A	7.63	0.35	A	9.77	0.48	A
	Spring	6.58	0.38	A	5.49	0.49	B	7.78	0.64	A
	Summer	7.71	0.40	A	7.90	0.43	A	8.85	0.61	A
$\delta^{13}C$	Winter	−21.59	0.18	A	−21.57	0.17	A	−21.99	0.23	A
	Spring	−23.26	0.23	B	−23.60	0.24	B	−22.94	0.30	A
	Summer	−23.47	0.24	B	−24.10	0.21	B	−22.61	0.28	A
$\delta^{15}N$	Winter	7.94	0.64	B	10.92	0.47	AB	9.38	0.59	A
	Spring	10.29	0.83	A	9.06	0.66	B	10.69	0.78	A
	Summer	11.23	0.88	A	12.41	0.59	A	12.04	0.74	A

Post hoc Tukey's HSD comparison tests ($P < 0.05$) were performed to identify statistical differences among seasonal means within each species (A > B).

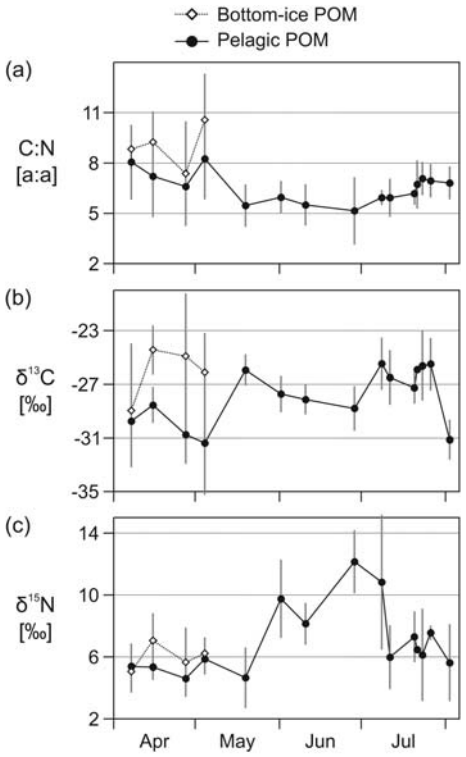

Fig. 8. Time series of **(a)** C:N ratio, **(b)** $\delta^{13}C$ and **(c)** $\delta^{15}N$ measured in POM sampled at the bottom of sea ice (when present, see Fig. 2a) and at the depth of the chlorophyll maximum (16–56 m) at ice break-up and in open water. The pelagic POM samples of early April when no chlorophyll maximum was observed in the water column were collected at 30 m depth.

Kosobokova, 2003). In the central Amundsen Gulf in 2008, ice algal production began in late March, peaked in mid-April, but the early ice melt in early May (usually early June; Galley *et al.*, 2008) potentially slowed down ice algae growth, thus leaving less time for zooplankton to harvest this food resource (S. Pineault, personal observation). Hence, it is probable that the shortage of ice algae in spring forced *C. glacialis* to use part of its lipid reserves for gonad maturation. This would explain why a significant decrease in the multiplier constant of the C–length equation of *C. glacialis* was observed in spring (Table III). Accordingly, the significantly low C:N ratio measured in this species in spring (Table VI) may reflect a low fatty acid content (as observed in *Calanus finmarchicus* by Mayor *et al.*, 2009). Contrary to *C. hyperboreus*, no statistical difference was found between the C–length equations of spring and summer in *C. glacialis*. Since this species can be found spawning from spring until the end of summer (Falk-Petersen *et al.*, 2009), a first explanation is that carbon gain through feeding in open water equalled their carbon losses allocated to egg production. Alternatively, the fact that *C. glacialis* females have been found at only a few stations in summer likely gave more weight to copepodite stages within the data set used to construct the C–length equation of summer.

Metridia longa is a well-known omnivore that stays active throughout the year (Conover and Huntley, 1991; Seuthe *et al.*, 2007) and that fuels its energy reserves via opportunistic feeding (e.g. Sampei *et al.*, 2009). In our study, the C–length relationships for this species were statistically similar, supporting the view that continuous ingestion on a variety of prey met its carbon demand over the seasons. Egg production studies in *M. longa* are scarce, but enhanced spawning in this species has been observed to be limited to the first 6 months of the year (Ashjian *et al.*, 2003 and references therein). In the Amundsen Gulf in 2008, *M. longa* began to produce eggs in late March (G. Darnis, personal observation). Interestingly, the individual C content of *M. longa* females increased from 180 to 280 μg C ind^{-1} from January to April, matching the beginning of its reproduction period (Fig. 5c). Since this increase in

C content coincided with the known time window of spawning by *C. hyperboreus*, we surmise that *M. longa* females were feeding on eggs produced at depth. Egg cannibalism by *M. longa* is increasingly recognized as a key component of its life cycle strategy (e.g. Ashjian *et al.*, 2003). Such predation behavior appears to enhance its own egg production rates (Plourde and Joly, 2008).

Our results show that lipid reserves in Arctic calanoids are most likely the major determinant of the differences among C contents and C–length relationships. Since we did not measure directly the lipid content in our study, we may use the mass balance model of Smyntek *et al.* (2007) to evaluate if any relations can be found between lipids and C contents. Using the fraction of lipid per body weight estimated via this model and our individual DW measurements (Fig. 3), it is possible to calculate the lipid content of each copepod. We present in Fig. 9 the linear regressions of the estimated lipid contents on the measured C contents for each species. Hence, the coefficients of determination (r^2) from these relationships can be seen as the variance of the C content explained by the lipid content. Accordingly, the variance of the C content was strongly explained by lipids in *C. hyperboreus* (93.7%) and *C. glacialis* (88.5%), while lipids were responsible for only 55.5% of the C content variability in *M. longa*. Therefore, these relations confirm that *M. longa* fed overall on a collection of prey less rich in fatty acids (e.g. detritus) and relies less on lipid reserves than the two large *Calanus* for its survival (see also Stevens *et al.*, 2004).

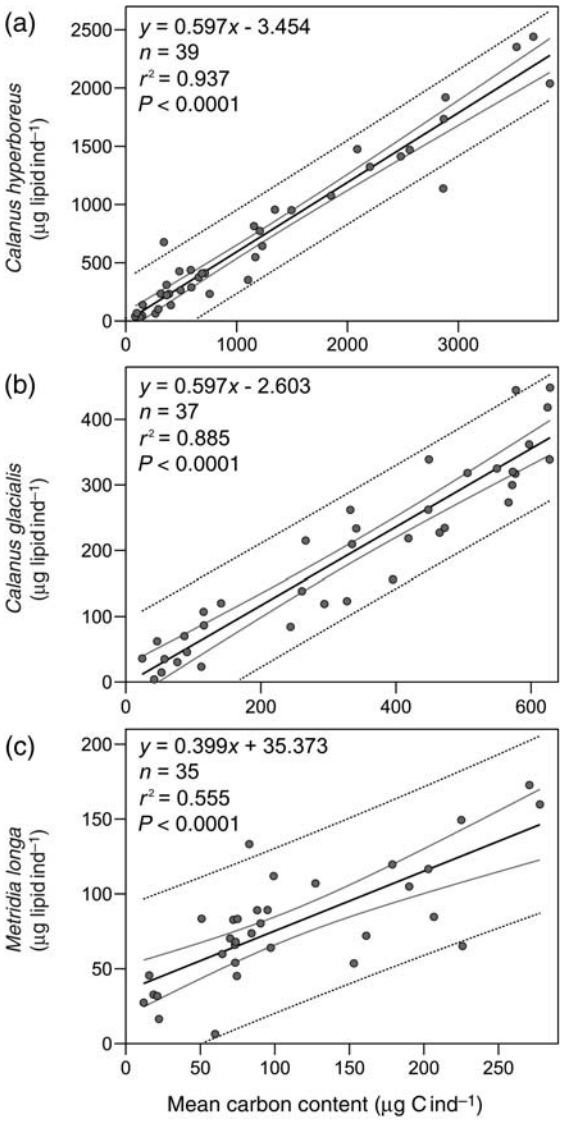

Fig. 9. Linear regressions of the individual lipid content (as estimated following Smyntek *et al.*, 2007) on the individual C content of each copepod species: **(a)** *C. hyperboreus*, **(b)** *C. glacialis* and **(c)** *M. longa*. The three relationships were built using the mean C content of each available stage at each sampling occasion.

The temporal shifts in the C:N ratio and stable isotopic composition of copepods and POM

In Arctic marine ecosystems, ice algal production starts in late winter when the region is ice-covered, but a rapid shift to phytoplankton production occurs as sea ice melts away (Carmack and Wassmann, 2006). This transition defines the spring bloom period when inorganic nutrients, which have been replenished in the surface layer during winter, are rapidly depleted when exposed to light (Sakshaug, 2004). Here, the sudden increase in chlorophyll biomass in May can be confidently linked to such pulsed-production pattern (Fig. 2b). Concomitant with this winter–spring transition, marked declines in the $\delta^{13}C$ and $\delta^{15}N$ of copepods were measured in every species (Fig. 7). The rapid depletion event observed in early April reflected the timing of herbivorous feeding, since the isotopic composition of copepods decreased suddenly to values close to those of POM. This suggests that all three calanoids exploited the new organic matter produced by ice algae because the biomass of chlorophyll fluorescence in the upper water column remained close to zero until late April (Fig. 2b). As the ice cover melted in early May, a switch to feeding on phytoplankton occurred as indicated by the ca. +4‰ increase in $\delta^{13}C$ recorded both in copepods and in pelagic POM (Figs 7d–f and 8b). In the North Water (NOW) polynya in 1998, the plankton samples most depleted in $\delta^{15}N$ and $\delta^{13}C$ were also collected in the early phase of the bloom when ice broke up (Tremblay *et al.*, 2006).

Contrary to the NOW polynya, inorganic nutrient inventories at the end of winter in the Beaufort Sea are low because of the strong stratification that isolates the surface layer from the deep nutrient-rich waters (Tremblay *et al.*, 2008). Nitrate limitation is known to induce a progressive ^{15}N enrichment of the nitrogen pool (Sigman and Casciotti, 2001). Such enrichment was observed in the pelagic POM at our sampling stations in May–June (Fig. 8c) and is obviously the main factor responsible for the increase in the $\delta^{15}N$ signal of copepods that occurred over spring. Similarly, the increase in the $\delta^{13}C$ values in May was likely induced by the phytoplankton uptake of dissolved inorganic carbon that had become progressively enriched in ^{13}C as a result of previous photosynthesis (e.g. Hinga *et al.*, 1994). Alternatively, active metabolic activities, production of tissue and excretion/egestion by copepods during enhanced growth periods might have for effect to enrich their bodies in ^{15}N and ^{13}C (Checkley and Entzeroth, 1985; Vanderklift and Ponsard, 2003; Tamelander *et al.*, 2006). The concomitant isotopic enrichment of copepods in spring thus supports that Arctic calanoids are adapted to match their growth with pulses of energy, such as phytoplankton blooms (Seuthe *et al.*, 2007; Falk-Petersen *et al.*, 2009; Søreide *et al.*, 2010). As a result, the peaks in the C:N ratio of copepods in late May/early June were presumably a result of the build-up of body reserves following the bloom (Koski, 1999). However, the drop in their C:N over June suggests that copepods lost part of their reserves during the period of low chlorophyll biomass (Fig. 2b). Such changes in the C:N ratio were more visible in *C. glacialis* and *M. longa* since these two species are smaller and have higher turnover/growth rates than *C. hyperboreus*. The lowest C contents in *M. longa* females and *C. glacialis* CV, two important stages in late spring (Table V), were also recorded in June (Fig. 5b and c). Interestingly, the temporal pattern of C:N ratio in copepods (Fig. 7a–c) seemed to be disconnected from fluctuations in the C:N ratio of POM (Fig. 8a), thus illustrating a decoupling in the stoichiometry between primary producers and consumers.

During summer, the C:N, $\delta^{13}C$ and $\delta^{15}N$ of copepods were less variable, but a comparable pattern to spring (i.e. a sequence of decrease–increase in these characteristics) can be noticed from late June to August. Although this shift is not as pronounced as in spring, this indicates that another bloom-like production occurred in the central Amundsen Gulf during this period. The increased chlorophyll concentrations recorded in summer (Fig. 2b) were actually linked to a second pulsed-production pattern that developed at depth (~50 m) in association with the nutricline. This "second" phytoplankton bloom was induced by the upward displacement of intermediate nutrient-rich waters in the central Amundsen Gulf as a consequence of wind-driven upwelling nearshore (J.-É. Tremblay, unpublished results). Accordingly, the sudden decrease in the $\delta^{15}N$ of pelagic POM in July is consistent with the further utilization of nitrate by micro-algae in the euphotic zone (Fig. 8c). The apparent rises in the C content and C:N ratio of copepods in late July likely mean that they recovered rapidly from the short starvation period of June (Figs 5 and 7a–c). Therefore, our results suggest that Arctic calanoid copepods respond rapidly to any increase in phytoplankton production and can cope with changes in the timing of primary production for building back their energy reserves.

In an attempt to characterize the trophic level of copepods during the two productive periods, Table VII presents the ^{15}N enrichment of each species using as a baseline the mean $\delta^{15}N$ values recorded at the bottom of sea ice and at the depth of chlorophyll maximum. Stepwise increase of $\delta^{15}N$ in marine food webs is usually 3–4‰ per trophic level (Michener and Schell, 1994). Here, only *C. hyperboreus* matched this range in spring-summer, indicating that only this species can be seen as a true herbivore over our study. The trophic ^{15}N enrichment in *M. longa* was slightly higher than +4‰ in both seasons. This modest shift suggests that *M. longa* was mainly feeding on phytoplankton, with occasional omnivory (as discussed above). The highest ^{15}N enrichment was yet observed in *C. glacialis* in summer, a period during which it also showed a mean $\delta^{15}N$ value statistically higher than in spring (Table VI). Such a pattern supports recent evidence that *C. glacialis* can also feed on microzooplankton when the latter are abundant as in summer (Campbell *et al.*, 2009).

Table VII: Mean trophic ^{15}N enrichment of each copepod species (stages CIV–V and adult females) in spring and summer using as a baseline the average $\delta^{15}N$ values of POM measured at the bottom of sea ice in early spring (7 April–4 May) and at the depth of the chlorophyll maximum at ice break-up and in open water (27 April–2 August)

		Mean trophic ^{15}N enrichment		
	Mean $\delta^{15}N$ of POM	*C. hyperboreus*	*Calanus glacialis*	*M. longa*
Spring	6.27‰	+4.01‰	+2.78‰	+4.41‰
Summer	7.76‰	+3.48‰	+4.65‰	+4.29‰

The discrete $\delta^{15}N$ values in bottom-ice and pelagic POM are presented in Fig. 8c.

In summary, the three copepods exhibited an herbivory signal in the Amundsen Gulf in spring-summer 2008 (Table VII), but the clear short-term variations (Fig. 7) indicate that vigilance should be exercised when calculating trophic levels. Moreover, whereas the food source of copepods in late spring and summer was manifestly of pelagic origin, it is difficult to quantify the exact fraction of their diet derived from ice algae flushed from sea ice in April/early May as standard deviations of biochemical properties of bottom-ice and pelagic POM were overlapping (Fig. 8).

The integrated C biomass and stage succession of dominant calanoid copepods in the Amundsen Gulf in 2008

Total mesozooplankton biomass estimated in studies conducted prior to 2006 across the Arctic Ocean rarely exceeded 5–6 g C m^{-2} (e.g. Thibault *et al.*, 1999; Ashjian *et al.*, 2003; Deibel and Daly, 2007; Kosobokova and Hirche, 2009; Kosobokova and Hopcroft, 2010). In the Amundsen Gulf region, previous measurements of mesozooplankton biomass over 2002–2004 were $\leq$4 g C m^{-2} (Darnis *et al.*, 2008; Forest *et al.*, 2008). In the present study, the large calanoid copepods *C. hyperboreus*, *C. glacialis* and *M. longa* alone yielded biomass estimates up to 7.6 and 9.7 g C m^{-2} in January and late July 2008, respectively. Hence, we suppose that the total mesozooplankton biomass could have been easily as high as 9–12 g C m^{-2} during these periods, a range even greater than in the highly productive NOW polynya in 1998 ($\leq$7.3 g C m^{-2}; Deibel and Daly, 2007). It is likely that enhanced growth and recruitment of mesozooplankton due to increased food resources and warm sea surface temperature can explain the high biomass of copepods in the Amundsen Gulf in 2008.

The spectacular retreat in Arctic sea ice in 2007 gave rise to a substantial increase in the growing season and primary production in the western Arctic Ocean, including the southeast Beaufort Sea (Arrigo *et al.*, 2008). Elevated water temperature and high food availability are expected to benefit zooplankton by enhancing their individual growth rates (Hirst and Bunker, 2003). Therefore, the biomass of copepods would have logically increased in 2007 in our study area. As a result, large populations of mesozooplankton have been sampled in January 2008 at the beginning of our investigation. In contrast, primary production in the European Arctic corridor decreased in 2007, when compared with 2006 (Arrigo *et al.*, 2008; Wassmann *et al.*, 2010). Simultaneously, a decline in the biomass of copepods was observed in the northern Barents Sea in late summer 2007, which was 3.6 times lower than in the previous year and dominated by small cyclopoids, not by large calanoids as it is usually the case (V. G. Dvoretsky, Murmansk Marine Biological Institute, personal communication). This simple comparison could mean that the magnitude of primary production cumulated over the growth season is a more important factor than its relative timing for the population development of Arctic calanoid copepods.

Furthermore, the negative trend in the total number of copepods from January to August has not been translated into a diminution of total C biomass (Fig. 6). This was mainly due to the numerical decline of young copepodite stages of *C. glacialis* and *M. longa* that has been compensated by an increased biomass of intermediate or adult stages of these species in spring–summer (Table V). In particular, the overwintering stages CIII–IV of *C. glacialis* moulted to CIV–V following the spring bloom in May and the remaining CIV moulted to CV in July as the second increase in phytoplankton biomass was detected. As a result, the C biomass summed for all three copepods in late summer (Fig. 6b) was dominated by *C. glacialis* CV at ca. 30%. According to Falk-Petersen *et al.* (Falk-Petersen *et al.*, 2009; see their Fig. 3), the succession of CIII to CV in *C. glacialis* in Arctic waters is supposed to occur over a 2-year period, whereas our results rather suggest a <1-year transition. Such a shift may reflect a high recruitment success following the appearance of young copepodite cohorts toward the end of the warm and more productive open-water season of 2007 (Arrigo *et al.*, 2008). This stage composition pattern could also explain the low standing stocks of *C. glacialis* females in 2008, since *C. glacialis* adults would be expected to be numerically abundant only after the overwintering of CV (Falk-Petersen *et al.*, 2009). Nevertheless, the fact that *C. glacialis* CI represented 29% of the abundance of this species in early August implies that notable egg spawning actually occurred in the previous months (as discussed above). Hence, naupliar development in *C. glacialis* probably took place in concomitance with the second pulse in phytoplankton production observed in July (cf. Søreide *et al.*, 2010).

Similar to *C. glacialis*, the rapid sequential dominances of CII–III to CIV and/or CV in the population of *M. longa* throughout our sampling period suggest a sufficient food supply to ensure the growth and development of this species. The continuous presence of *M. longa* CI from January to August supports as well the maintenance of favorable recruitment conditions in 2008. Also clearly observable, the first counts of *C. hyperboreus* CI–II were made in late winter (March) and a rapid succession from CIV to CV in the total abundance of this species was detected over the

phytoplankton bloom period in May (Table V). In comparison, an advanced recruitment of calanoid copepods was deduced in the NOW polynya in 1998 on the basis of first CI–III observed in May–June (Ringuette *et al.*, 2002). Hence, our results could indicate that the population development of calanoid copepods was even more rapid in the Amundsen Gulf in 2008 than in the NOW polynya in 1998. Even if we cannot firmly conclude on such statement, the positive trend in total copepod biomass from April to August suggests that the early ice melt and the successive pulses in micro-algal resources in spring-summer resulted in a sustained secondary production.

CONCLUSIONS

The temporal changes in the elemental and stable isotopic composition of *C. hyperboreus*, *C. glacialis* and *M. longa* observed in this study reflected the various life-history strategies that co-exist among Arctic calanoids. We thus provide specific relationships between C content and prosome length that account for the different metabolic, feeding and reproductive behaviors of these dominant copepod species. This should enable more precise estimates of their biomass in the southeast Beaufort Sea. In addition, the substantial $\delta^{13}C$ and $\delta^{15}N$ variations measured in all three species during bloom-like events illustrated their rapid response to pulsed phytoplankton production. It is likely that such episodic enrichment in the isotopic composition of key zooplankton species will be transferred to higher trophic levels (e.g. Loseto *et al.*, 2008). Future analyses of food web interactions in the Beaufort Sea ecosystem should therefore be cautious and consider these marked variations in the estimation of trophic levels.

Since the data used in our study were acquired during a year of early ice break-up and following the 2007 record low in Arctic sea ice (Wang and Overland, 2009; NSIDC, 2010), our results may already mirror an ecosystem in transition. The high copepod biomass measured in the Amundsen Gulf in 2008 was probably the result of the enhanced primary production and increased sea surface temperature observed in 2007 over the Arctic Amerasian shelves (Arrigo *et al.*, 2008). The simultaneous response of copepods to an early spring bloom and sustained productivity in summer (as inferred from their biochemical composition and population development) illustrated overall their capacity to cope with environmental changes. This aptitude is presumably a consequence of their inherent plasticity in dealing with various physical gradients and food regimes (e.g. Conover and Huntley, 1991; Deibel and Daly, 2007; Falk-Petersen *et al.*, 2009). We conclude that dominant Arctic calanoid copepods in the southeast Beaufort Sea may continue to benefit from a longer season of pelagic primary production as induced by climate warming in high northern latitudes. However, the monitoring of key zooplankton species is a critical task as thresholds associated with more intense interspecific competition or negative shifts in the food quantity/quality are possible in the context of ongoing rapid changes.

ACKNOWLEDGEMENTS

We express high gratitude to the officers and crew members of the CCGS *Amundsen* for professional and enthusiastic assistance at sea. We thank L. Létourneau, M. Sampei, J. Michaud, M. Ringuette, C. Bouchard, J. Gagné, S. Thanassekos, H. Cloutier and B. Robineau for help at sea and/or in the laboratory. Special thanks to Y. Gratton, P. Massot and D. Boisvert for the processing of the CTD data and to J. Martin for the calibration factors of the fluorometer probe. We thank the coordinators of the Circumpolar Flaw Lead (CFL) System Study D. Leitch and M. Pucko for the organization of the fieldwork and workshops. We gratefully thank two anonymous reviewers for insightful comments that strengthened and greatly improved the initial manuscript. The writing of this paper has been initiated during a postdoctoral stay at the University of Tromsø, Norway, and AF would like to thank Paul Wassmann for the hospitality.

FUNDING

The CFL System Study is a project of the International Polar Year (IPY) 2007–2008 financially supported by the Government of Canada (IPY #96). A.F. benefited from postdoctoral scholarships from the Fonds québécois de la recherche sur la nature et les technologies and from the Natural Sciences and Engineering Research Council of Canada. This work is a joint contribution to the research programs of CFL-IPY, Québec-Océan, to the ArcticNet Network of Centres of Excellence of Canada and to the Canada Research Chair on the response of marine Arctic ecosystems to climate warming.

REFERENCES

Arashkevich, E., Wassmann, P., Pasternak, A. *et al.* (2002) Seasonal and spatial changes in biomass, structure, and development

progress of the zooplankton community in the Barents Sea. *J. Mar. Syst.*, **38**, 125–145.

Arrigo, K. R. and van Dijken, G. L. (2004) Annual cycles of sea ice and phytoplankton in Cape Bathurst polynya, southeastern Beaufort Sea, Canadian Arctic. *Geophys. Res. Lett.*, **31**, L08304.

Arrigo, K. R., van Dijken, G. and Pabi, S. (2008) Impact of a shrinking Arctic ice cover on marine primary production. *Geophys. Res. Lett.*, **35**, L19603.

Ashjian, C. J., Campbell, R. G., Welch, H. E. *et al.* (2003) Annual cycle in abundance, distribution, and size in relation to hydrography of important copepod species in the western Arctic Ocean. *Deep-Sea Res. I*, **50**, 1235–1261.

Barber, D. (2009) *Circumpolar Flaw Lead System Study (CFL)—International Polar Year (IPY)—CCGS Amundsen*. 27 September 2007–7 August 2008, Scientific Cruise Reports Compendium. http://www.ipy-cfl.ca/page1/page21/page21.html

Benoit, D., Simard, Y., Gagné, J. *et al.* (2010) From polar night to midnight sun: photoperiod, seal predation, and the diel vertical migrations of polar cod (*Boreogadus saida*) under landfast ice in the Arctic Ocean. *Polar Biol.* doi: 10.1007/s00300-010-0840-x

Campbell, R. G., Sherr, E. B., Ashjian, C. J. *et al.* (2009) Mesozooplankton prey preference and grazing impact in the Western Arctic Ocean. *Deep-Sea Res. II*, **56**, 1274–1289.

Carmack, E. and Wassmann, P. (2006) Food webs and physical-biological coupling on pan-Arctic shelves: Unifying concepts and comprehensive perspectives. *Prog. Oceanogr.*, **71**, 446–477.

Checkley, D. M. Jr and Entzeroth, L. C. (1985) Elemental and isotopic fractionation of carbon and nitrogen by marine, planktonic copepods and implications to the marine nitrogen cycle. *J. Plankton Res.*, **7**, 553–568.

Conover, R. J. and Huntley, M. (1991) Copepods in ice-covered seas—distribution, adaptations to seasonally limited food, metabolism, growth patterns and life cycle strategies in polar seas. *J. Mar. Syst.*, **2**, 1–41.

Crease, J. (1988) *The Acquisition, Calibration and Analysis of CTD Data. UNESCO Technical Papers in Marine Science No. 54. (A Report of SCOR Working Group 51)*. Division of Marine Sciences, UNESCO, Paris, France.

Darnis, G., Barber, D. G. and Fortier, L. (2008) Sea ice and the onshore–offshore gradient in pre-winter zooplankton assemblages in south-eastern Beaufort Sea. *J. Mar. Syst.*, **74**, 994–1011.

Deibel, D. and Daly, K. (2007) Zooplankton processes in Arctic and Antarctic polynyas. In Smith, W. O. and Barber, D. G. (eds), *Polynyas: Windows to the World*. Elsevier, Amsterdam, pp. 271–311.

Drinkwater, K. F., Beaugrand, G., Kaeriyama, M. *et al.* (2010) On the processes linking climate to ecosystem changes. *J. Mar. Syst.*, **79**, 374–388.

Falk-Petersen, S., Mayzaud, P., Kattner, G. *et al.* (2009) Lipids and life strategy of Arctic *Calanus*. *Mar. Biol. Res.*, **5**, 18–39.

Forest, A., Sampei, M., Makabe, R. *et al.* (2008) The annual cycle of particulate organic carbon export in Franklin Bay (Canadian Arctic): environmental control and food web implications. *J. Geophys. Res.*, **113**, C03S05.

Forest, A., Bélanger, S., Sampei, M. *et al.* (2010) Three-year assessment of particulate organic carbon fluxes in Amundsen Gulf (Beaufort Sea): satellite observations and sediment trap measurements. *Deep-Sea Res. I*, **57**, 125–142.

Fortier, M., Fortier, L., Michel, C. *et al.* (2002) Climatic and biological forcing of the vertical flux of biogenic particles under seasonal Arctic sea ice. *Mar. Ecol. Prog. Ser.*, **225**, 1–16.

Frost, B. W. (1974) *Calanus marshallae*, a new species of calanoid copepod closely allied to the sibling species *C. finmarchicus* and *C. glacialis*. *Mar. Biol.*, **26**, 77–99.

Galley, R. J., Key, E., Barber, D. G. *et al.* (2008) Spatial and temporal variability of sea ice in the southern Beaufort Sea and Amundsen Gulf: 1980–2004. *J. Geophys. Res.*, **113**, C05S95.

Garrison, D. and Buck, K. (1986) Organism losses during ice melting: a serious bias in sea ice community studies. *Polar Biol.*, **6**, 237–239.

Head, E. J. H., Harris, L. R. and Abou Debs, C. (1985) Effect of daylength and food concentration on in situ diurnal feeding rhythms in Arctic copepods. *Mar. Ecol. Prog. Ser.*, **24**, 281–288.

Hinga, K. R., Arthur, M. A., Pilson, M. E. Q. *et al.* (1994) Carbon isotope fractionation by marine phytoplankton in culture: the effects of CO_2 concentration, pH, temperature, and species. *Global Biogeochem. Cycles*, **8**, 91–102.

Hirche, H. J. and Kosobokova, K. (2003) Early reproduction and development of dominant calanoid copepods in the sea ice zone of the Barents Sea—need for a change of paradigms? *Mar. Biol.*, **143**, 769–781.

Hirst, A. G. and Bunker, A. J. (2003) Growth of marine planktonic copepods: global rates and patterns in relation to chlorophyll a, temperature, and body weight. *Limnol. Oceanogr.*, **48**, 1988–2010.

Hopcroft, R. R., Clarke, C., Nelson, R. J. *et al.* (2005) Zooplankton communities of the Arctic's Canada Basin: the contribution by smaller taxa. *Polar Biol.*, **28**, 198–206.

Ingram, R. G., Williams, W. J., van Hardenberg, B. *et al.* (2008) Seasonal circulation over the Canadian Beaufort Shelf. In Fortier, L., Barber, D. G. and Michaud, J. (eds), *On Thin Ice: A Synthesis of the Canadian Arctic Shelf Exchange Study (CASES)*. Aboriginal Issues Press, Winnipeg, pp. 13–38.

Kosobokova, K. and Hirche, J. (2009) Biomass of zooplankton in the eastern Arctic Ocean—a base line study. *Prog. Oceanogr.*, **82**, 265–280.

Kosobokova, K. N. and Hopcroft, R. R. (2010) Diversity and vertical distribution of mesozooplankton in the Arctic's Canada Basin. *Prog. Oceanogr.*, **57**, 96–110.

Koski, M. (1999) Short communication. Carbon:nitrogen ratios of Baltic Sea copepods—indication of mineral limitation? *J. Plankton Res.*, **21**, 1565–1573.

Logan, J. M., Jardine, T. D., Miller, T. J. *et al.* (2008) Lipid corrections in carbon and nitrogen stable isotope analyses: comparison of chemical extraction and modelling methods. *J. Anim. Ecol.*, **77**, 838–846.

Loseto, L. L., Stern, G. A., Deibel, D. *et al.* (2008) Linking mercury exposure to habitat and feeding behaviour in Beaufort Sea beluga whales. *J. Mar. Syst.*, **74**, 1012–1024.

Madsen, S. D., Nielsen, T. G. and Hansen, B. W. (2001) Annual population development and production by *Calanus finmarchicus*, *C. glacialis* and *C. hyperboreus* in Disko Bay, western Greenland. *Mar. Biol.*, **139**, 75–93.

Magen, C., Chaillou, G., Crowe, S. A. *et al.* (2010) Origin and fate of particulate organic matter in the southern Beaufort Sea–Amundsen Gulf region, Canadian Arctic. *Estuar. Coast. Shelf Sci.*, **86**, 31–41.

Markus, T., Stroeve, J. C. and Miller, J. (2009) Recent changes in Arctic sea ice melt onset, freezeup, and melt season length. *J. Geophys. Res.*, **114**, C12024.

Mayor, D. J., Anderson, T. R., Pond, D. W. *et al.* (2009) Egg production and associated losses of carbon, nitrogen and fatty acids from maternal biomass in *Calanus finmarchicus* before the spring bloom. *J. Mar. Syst.*, **78**, 505–510.

Michener, R. and Schell, D. (1994) Stable isotope ratios as tracers in marine aquatic food webs. In Lajtha, K. and Michener, R. (eds), *Stable Isotopes in Ecology and Environmental Science*. Blackwell Scientific Publications, Oxford, pp. 138–157.

Morata, N., Renaud, P. E., Brugel, S. *et al.* (2008) Spatial and seasonal variations in the pelagic-benthic coupling of the southeastern Beaufort Sea revealed by sedimentary biomarkers. *Mar. Ecol. Prog. Ser.*, **371**, 47–63.

Mumm, N. 1991 On the summerly distribution of mesozooplankton in the Nansen Basin, Arctic Ocean (in German). *Rep. Polar Mar. Res.*, **92**, 1–173. http://hdl.handle.net/10013/epic.10092

NSIDC. (2010) National Snow and Ice Data Center—Arctic Sea Ice News and Analysis Web Page, updated continuously. http://nsidc.org/arcticseaicenews/

Plourde, S. and Joly, P. (2008) Comparison of *in situ* egg production rate in *Calanus finmarchicus* and *Metridia longa*: discriminating between methodological and species-specific effects. *Mar. Ecol. Prog. Ser.*, **353**, 165–175.

Qi, H., Coplen, T. B., Geilmann, H. *et al.* (2003) Two new organic reference materials for delta13C and delta15N measurements and a new value for the delta13C of NBS 22 oil. *Rapid Commun. Mass Spectrom.*, **17**, 2483–2487.

Ringuette, M., Fortier, L., Fortier, M. *et al.* (2002) Advanced recruitment and accelerated population development in Arctic calanoid copepods of the North Water. *Deep-Sea Res. II*, **49**, 5081–5099.

Runge, J. A. and Ingram, R. G. (1991) Under-ice feeding and diel migration by the planktonic copepods *Calanus glacialis* and *Pseudocalanus minutus* in relation to the ice algal production cycle in southeastern Hudson Bay, Canada. *Mar. Biol.*, **108**, 217–225.

Sakshaug, E. (2004) Primary and secondary production in the Arctic Seas. In Stein, R. and MacDonald, R. W. (eds), *The Organic Carbon Cycle in the Arctic Ocean*. Springer-Verlag, New York, pp. 57–81.

Sampei, M., Forest, A., Sasaki, H. *et al.* (2009) Attenuation of the vertical flux of copepod fecal pellets under Arctic sea ice: evidence for an active detrital food web in winter. *Polar Biol.*, **32**, 225–232.

Seuthe, L., Darnis, G., Riser, C. W. *et al.* (2007) Winter–spring feeding and metabolism of Arctic copepods: insights from faecal pellet production and respiration measurements in the southeastern Beaufort Sea. *Polar Biol.*, **30**, 427–436.

Sigman, D. M. and Casciotti, K. L. (2001) Nitrogen isotopes in the ocean. In Steele, J. H., Turekian, K. K. and Thorpe, S. A. (eds), *Encyclopedia of Ocean Sciences*. Academic Press, San Diego, pp. 1884–1894.

Smith, S. L. and Schnack-Schiel, S. B. (1990) Polar zooplankton. In Smith, W. O. and Barber, D. G. (eds), *Polar Oceanography, Part B Chemistry, Biology, and Geology*. Academic Press, San Diego, pp. 527–598.

Smyntek, P. M., Teece, M. A., Schulz, K. L. *et al.* (2007) A standard protocol for stable isotope analysis of zooplankton in aquatic food web research using mass balance correction models. *Limnol. Oceanogr.*, **52**, 2135–2146.

Sokal, R. R. and Rohlf, F. J. (1995) *Biometry: The Principles and Practice of Statistics in Biological Research*. WH Freeman, New York.

Søreide, J. E., Falk-Petersen, S., Hegseth, E. N. *et al.* (2008) Seasonal feeding strategies of *Calanus* in the high-Arctic Svalbard region. *Deep-Sea Res. II*, **55**, 2225–2244.

Søreide, J. E., Leu, E., Berge, J. *et al.* (2010) Timing of blooms, algal food quality and *Calanus glacialis* reproduction and growth in a changing Arctic. *Global Change Biol.* doi: 10.1111/j.1365-2486.2010.02175.x

Stevens, C. J., Deibel, D. and Parrish, C. C. (2004) Species-specific differences in lipid composition and omnivory indices in Arctic copepods collected in deep water during autumn (North Water polynya). *Mar. Biol.*, **144**, 905–915.

Sweeting, C. J., Polunin, N. V. C. and Jennings, S. (2006) Effects of chemical lipid extraction and arithmetic lipid correction on stable isotope ratios of fish tissues. *Rapid Commun. Mass Spectrom.*, **20**, 595–601.

Tamelander, T., Søreide, J., Hop, H. *et al.* (2006) Fractionation of stable isotopes in the Arctic marine copepod *Calanus glacialis*: Effects on the isotopic composition of marine particulate organic matter. *J. Exp. Mar. Biol. Ecol.*, **333**, 231–240.

Thibault, D., Head, E. J. H. and Wheeler, P. A. (1999) Mesozooplankton in the Arctic Ocean in summer. *Deep-Sea Res. I*, **46**, 1391–1416.

Tremblay, J. E., Michel, C., Hobson, K. A. *et al.* (2006) Bloom dynamics in early opening waters of the Arctic Ocean. *Limnol. Oceanogr.*, **51**, 900–912.

Tremblay, J. E., Simpson, K., Martin, J. *et al.* (2008) Vertical stability and the annual dynamics of nutrients and chlorophyll fluorescence in the coastal, southeast Beaufort Sea. *J. Geophys. Res.*, **113**, C07S90.

van de Waal, D. B., Verschoor, A. M., Verspagen, J. M. H. *et al.* (2009) Climate-driven changes in the ecological stoichiometry of aquatic ecosystems. *Front. Ecol. Environ.* e-View, doi: 10.1890/080178

Vanderklift, M. and Ponsard, S. (2003) Sources of variation in consumer-diet 15N enrichment: a meta-analysis. *Oecologia*, **136**, 169–182.

Wang, M. and Overland, J. E. (2009) A sea ice free summer Arctic within 30 years? *Geophys. Res. Lett.*, **36**, L07502.

Wassmann, P., Slagstad, D. and Ellingsen, I. (2010) Primary production and climatic variability in the European sector of the Arctic Ocean prior to 2007: preliminary results. *Polar Biol.* doi: 10.1007/s00300-010-0839-3

Wiafe, G., Yaqub, H. B., Mensah, M. A. *et al.* (2008) Impact of climate change on long-term zooplankton biomass in the upwelling region of the Gulf of Guinea. *ICES J. Mar. Sci.*, **65**, 318–324.